Electron microscopic observation of cytoskeletal frame structures and detection of tubulin on the apical region of *Cryptosporidium parvum* sporozoites

M. MATSUBAYASHI[1], H. TAKASE[2], I. KIMATA[3], H. NAKAGAWA[4], H. TANI[5], K. SASAI[5]* *and* E. BABA[5]

[1] *Department of Food and Nutrition, Osaka Yuhigaoka Gakuen Junior College, Tennoji-ku, Osaka 543-0073, Japan*
[2] *Hanaichi Ultrastructure Research Institute, Okazaki, Aichi 444-0076, Japan*
[3] *Department of Protozoal Diseases, Graduate School of Medicine, Osaka City University, Abeno-ku, Osaka 545-8585, Japan*
[4] *Department of Central Laboratory, Graduate School of Medicine, Osaka City University, Abeno-ku, Osaka 545-8585, Japan*
[5] *Department of Veterinary Internal Medicine, Division of Veterinary Science, Graduate School of Life and Environmental Sciences, Osaka Prefecture University, Sakai, Osaka 599-8531, Japan*

(*Received 25 June 2007; revised 21 August and 11 September 2007; accepted 26 September 2007; first published online 27 November 2007*)

SUMMARY

Cryptosporidium parvum is an intracellular protozoan parasite belonging to the phylum Apicomplexa, and a major cause of waterborne gastroenteritis throughout the world. Invasive zoites of apicomplexan parasites, including *C. parvum*, are thought to have characteristic organelles on the apical apex; however, compared with other parasites, the cytoskeletal ultrastructure of *C. parvum* zoites is poorly understood. Thus, in the present study, we ultrastructurally examined *C. parvum* sporozoites using electron microscopy to clarify the framework of invasive stages. Consequently, at the apical end of sporozoites, 3 apical rings and an electron-dense collar were seen. Two thick central microtubules were seen further inside sporozoites and extended to the posterior region. Using anti-α and -β tubulin antibodies generated from sea urchin and rat brain, both antibodies cross-reacted at the apical region of sporozoites in immunofluorescent morphology. The molecular mass of *C. parvum* α tubulin antigen was 50 kDa by Western blotting and the observed apical cytoskeletal structures were shown to be composed of α tubulin by immunoelectron microscopy. These results suggested that *C. parvum* sporozoites were clearly different in their cytoskeletal structure from those of other apicomplexan parasites.

Key words: apicalcomplex, *Cryptosporidium*, cytoskeleton, sporozoite, tubulin.

INTRODUCTION

Protozoa infection of the phylum Apicomplexa including *Plasmodium* spp., *Toxoplasma gondii*, *Eimeria* spp. and *Cryptosporidium* spp. occurs worldwide in humans and animals (Black and Boothroyd, 2000; Xiao *et al*. 2004; Daugschies and Najdrowski, 2005; Ashley *et al*. 2006; Morris and Gasser, 2006). These parasites, which are obligate intracellular parasites, have complex life-cycles involving transmission, and invade, grow and replicate within host cells. Invasive zoites of apicomplexa parasites possess unique organelles called the apical complex which play an important role in its motility and/or invasion into host cells. This apical complex is generally composed of rhoptries, micronemes and dense granules, which are secretory organelles (Sam-Yellowe, 1996), and apical or polar rings, conoid and subpellicular microtubules, which provide a cytoskeletal framework during host cell invasion (Lindsay *et al*. 1991, 1993; Hu *et al*. 2002). It has been thought that microtubules composed of polymers of α and β tubulins form these cytoskeletal frames of zoites, such as conoid as well as subpellicular microtubules.

C. parvum is an intracellular protozoa belonging to the phylum Apicomplexa, and is a common cause of waterborne gastroenteritis throughout the world in animals and humans (O'Donoghue, 1995; Chen *et al*. 2002). In immunocompetent patients, *C. parvum* develop a self-limited watery diarrhoea lasting 1–2 weeks; however, the disease can be life-threatening in immunodeficient patients, such as those with acquired immunodeficiency syndrome (AIDS) (O'Donoghue, 1995; Chen *et al*. 2002). Despite the magnitude and severity of *C. parvum* infections, there are no effective pharmaceutical therapies or immunotherapy, including approved vaccines (O'Donoghue, 1995; Perryman *et al*. 1999; Sagodira *et al*. 1999; Chen *et al*. 2002).

Like other apicomplexan parasites, the invasive form (sporozoite or merozoite) of *C. parvum* is thought to possess characteristic apical organelles.

* Corresponding author: Department of Veterinary Internal Medicine, Division of Veterinary Science, Graduate School of Life and Environmental Sciences, Osaka Prefecture University, Sakai, Osaka 599-8531, Japan. Tel: +81 72 254 9506. Fax: +81 72 254 9918. E-mail: ksasai@vet.osakafu-u.ac.jp

Parasitology (2008), **135**, 295–301.
doi:10.1017/S003118200700385X Printed in the United Kingdom

Recent morphological studies using electron microscopy have revealed that *C. parvum* sporozoites have a single rhoptry, multiple micronemes and dense granules around the apical region (Tetley *et al.* 1998); however, compared with these secretory organelles, the cytoskeletal structure of *C. parvum* zoites has not been fully analysed. So far, genes encoding tubulins of *C. parvum* have been characterized genetically (Bonafonte *et al.* 1999; Hu *et al.* 2002; Abrahamsen *et al.* 2004); furthermore, anti-microtubule drugs which can disrupt the microtubule network within sporozoites inhibit *C. parvum* infection of host cells (Wiest *et al.* 1994). These findings, in previous studies, proved that cytoskeletal organelles, especially microtubules, were present on *C. parvum* zoites and related with the host cell invasion of *C. parvum*; however, these morphological frame structures of *C. parvum* zoites remain unclear. Thus, in the present study, we morphologically examined *C. parvum* sporozoites using electron or immunoelectron microscopy to clarify the ultrastructural frames of invasive stages.

MATERIALS AND METHODS

Parasites

C. parvum oocysts, strain HNJ-1, were originally obtained from the faeces of a patient in Japan (Abe *et al.* 2002). These oocysts were passaged in severe combined immunodeficient (SCID) mice, purified by the sugar flotation method, and stored at 4 °C in phosphate-buffered saline (PBS, pH 7·2) until 1 month before use, or were freeze-dried for Western blot analysis. *C. parvum* sporozoites were prepared as previously reported except for using RPMI medium 1640 (Invitrogen) (Matsubayashi *et al.* 2005).

Transmission electron microscopy (TEM)

The *C. parvum* sporozoites prepared as described above were fixed with 2% glutaraldehyde (GA, Electron Microscopy Sciences) and 1% tannic acid (Wako Pure Chemical Industries Ltd) in 0·1 M phosphate buffer (PB, pH 7·4) at room temperature for 2 h, additionally fixed with 2% GA at 4 °C for 1 week, and washed in 0·1 M PB. They were post-fixed with 2% OsO_4 in 0·1 M PB at 4 °C for 2–3 h, dehydrated in an ethanol series and embedded in Epon resin. Ultra-thin sections were stained with 2% uranyl acetate (Cerac Inc.) in distilled water for 15 min, lead staining solution (Hanaichi *et al.* 1986) for 5 min, and examined with an electron microscope (JEM-1200, JEOL).

Negative staining

Extraction by Triton X-100 was performed to reveal the detailed organization of the cytoskeleton (Nichols and Chiappino, 1987). Briefly, 10^6 *C. parvum* sporozoites, excysted as described above, were suspended in 0%, 0·1% or 0·5% Triton X-100 (Sigma-Aldrich Co.) in RPMI medium 1640 (Invitrogen) for 5–10 min, fixed in 0·1% GA (TAAB Laboratories Equipment Ltd) and 2% paraformaldehyde (PFA, Merck Ltd) in 0·1 M PB at 4 °C for 4–6 days, and washed in ultra-pure water (UPW). Five μl of parasite suspension, resuspended in 400 μl of UPW, were dropped onto carbon-stabilized 200-mesh nickel grids (Nissin EM Co. Ltd) covered with thin collodion film (Nissin EM Co. Ltd), and allowed to settle for 20 min in a humid chamber. Excess fluid was removed and the grids were air-dried. The parasites on the grids were stained with 2% phosphotungstic acid (PTA, pH 7·5, TAAB Laboratories Equipment Ltd) or 1% uranyl acetate (TAAB Laboratories Equipment Ltd) for 30 sec and examined with an electron microscope (H-7500, Hitachi).

Indirect immunofluorescence assay (IFA)

For IFA with *C. parvum* sporozoites, slides were prepared as previously reported (Matsubayashi *et al.* 2005), fixed using methanol, acetone or 0·05% GA and 2% PFA for 10 min or non-fixed, and stored at −80 °C until use. Parasites fixed with 0·05% GA and 2% PFA were blocked with 0·1 M glycine (Nacalai Tesque) in PBS before immunostaining. After washing and drying, prepared slides were treated with 0%, 0·1% or 1% Triton X-100 in PBS for 10 min and washed 3 times for 5 min in PBS. After blocking with 1% bovine serum albumin (BSA, Sigma-Aldrich Co.) in PBS for 10 min, the slides were incubated with 50 μl of primary antibody, mouse anti-α tubulin (monoclonal, against the C-terminal region of α tubulin isoform derived from sea urchin sperm axonemes; T5168, Sigma-Aldrich Co.) at 1 : 1000 dilution or mouse anti-β tubulin (monoclonal, against purified rat brain tubulin; T4026, Sigma-Aldrich Co.) at 1 : 500 dilution in 1% BSA in PBS for 40 min. As a control, purified normal mouse IgG (Sigma-Aldrich Co.) at 1 : 1000 dilution was used. The slides were washed 3 times with PBS containing 0·05% Tween 20 (PBST) and incubated with 50 μl of fluorescein isothiocyanate (FITC)-conjugated rabbit anti-mouse IgG at 1 : 100 dilution (Sigma-Aldrich Co.) for 30 min. After immunostaining, the slides were mounted with 50% glycerol (Nacalai Tesque) in PBS for examinations using an epi-fluorescent microscope (Nikon). All steps were performed at room temperature.

Western blot analysis

For analyses by sodium dodecyl sulfate-polyacrylamide gel electrophoresis (SDS-PAGE) and Western blotting, *C. parvum* oocyst antigen was prepared as

https://doi.org/10.1017/S003118200700385X Published online by Cambridge University Press

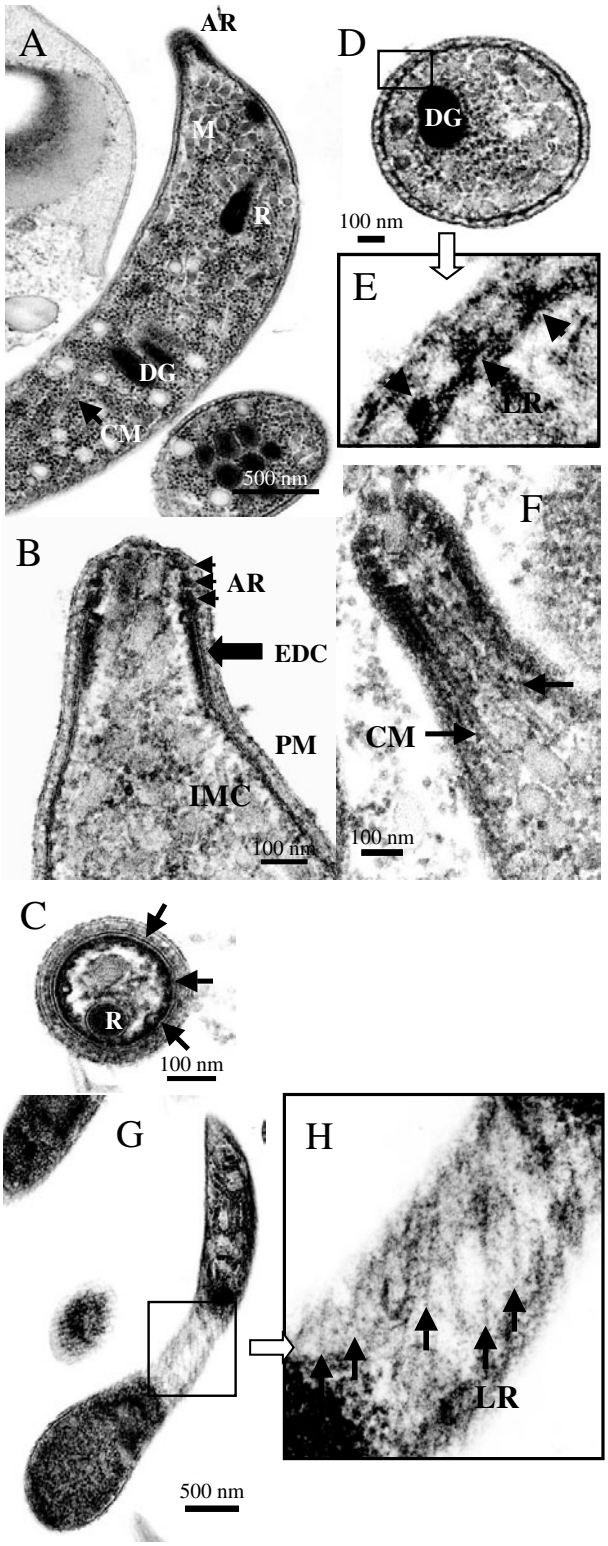

Fig. 1. Transmission electron micrographs of *Cryptosporidium parvum* sporozoites. (A) Traverse section of the anterior region of a sporozoite. Only a single rhoptry was seen in *C. parvum* sporozoites. (B) Higher magnification of the sporozoite anterior region. Small arrows show apical rings and the large arrow shows the electron-dense collar. (C) Cross-section of the apical end of the sporozoite. Arrows show the electron-dense collar beneath the inner membrane complex. (D) Cross-section at middle region of the sporozoite. Longitudinal ridges are present between the plasma membrane and inner membrane complex and run as a spiral around the sporozoite (DG). (E and H) High magnifications of the boxed regions in (D) and (G), respectively. Arrows show longitudinal ridges. (F) Higher magnification of the anterior region of the sporozoite. Arrows show 2 thick central microtubules. AR, Apical rings; EDC, electron-dense collar; PM, plasma membrane; IMC, inner membrane complex; CM, central microtubules; LR, longitudinal ridges; R, rhoptry; M, micronemes; DG, dense granules.

previously reported (Matsubayashi *et al.* 2005). Briefly, 20 μg of *C. parvum* oocysts antigens were resolved on 4% stacking/12% resolving SDS-PAGE at 200 V constant voltage (Laemmli, 1970) and the separated proteins were blotted to PVDF membrane (Immobilon Transfer Membranes, Millipore). After blocking with 1% BSA in PBS, membranes of blotted individual lanes were stained for 1 h at room temperature with anti-α tubulin antibody at 1 : 1000 dilution, anti-β tubulin antibody at 1 : 100 dilution or normal mouse IgG at 1 : 1000 dilution as a control in 1% BSA in PBS, and washed 3 times for 5 min with PBST. Bound antibodies were detected by staining with horseradish peroxidase-labelled goat anti-mouse IgG Fab specific (Sigma-Aldrich Co.) at 1 : 10000 dilution for 1 h and developed with Konica Immunostaining HRP-1000 (Konica). Molecular weights were estimated using standard molecular weight proteins after staining with 0·2% Coomassie Brilliant Blue R-250 (Wako Pure Chemical Industries Ltd).

Two-dimensional polyacrylamide gel electrophoresis (2-DE)

Two-dimensional polyacrylamide gel electrophoresis was performed using Protean IEF Cell (Bio-Rad) according to the manufacturer's protocol. Briefly, 10^9 freeze-dried *C. parvum* oocysts were dissolved in 1 ml of the Rehydration/Sample buffer (Bio-Rad), which contained 8 M urea, 2% CHAPS, 50 mM dithiothreitol (DTT), 0·2% Bio-lyte 3/10, and 0·001% bromophenol blue, sonicated in an ice bath with an Ultrasonic Processor (Taitec Co.) and centrifuged at 600 ***g*** for 5 min. The supernatant was aliquoted and cryopreserved at −80 °C until use. The concentration of crude antigen was determined by Coomassie Blue Assay Kit (Pierce). For first-dimensional electrophoresis, ReadyStrip^{TM} pH 3–10 IPG strips (7 cm; Bio-Rad) were rehydrated by loading Rehydration/Sample buffer containing 20 μg of prepared antigen for 12 h. After rehydration, focussing conditions were 20 min at 250 V to remove excess salts, 2 h at 4000 V for voltage ramping, followed by focussing for 2·5 h at 4000 V. The temperature was set at 20 °C. After isoelectric focussing, strips were laid onto 4% stacking/12% gradient SDS-PAGE gels and resolved in the

https://doi.org/10.1017/S003118200700385X Published online by Cambridge University Press

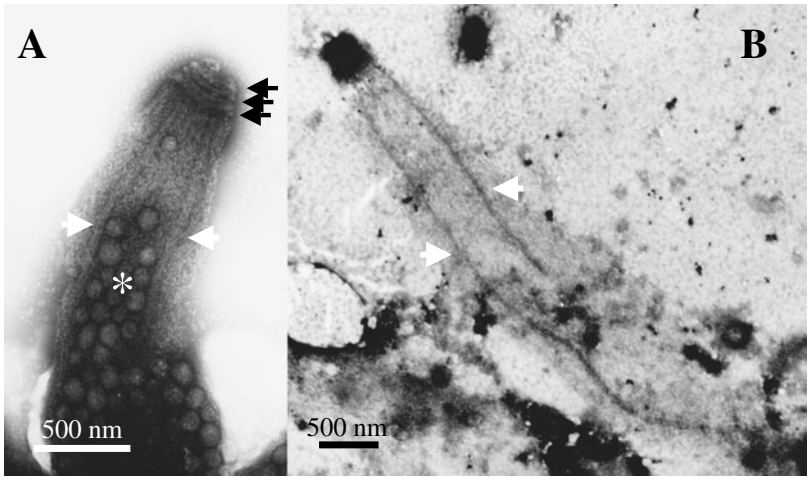

Fig. 2. Electron micrographs of *Cryptosporidium parvum* sporozoites treated with 0·1% Triton X-100 for 5 min. Detergent-treated sporozoites are negatively stained by 2% phosphotungstic acid (A) or 1% uranyl acetate (B). Black arrows and an asterisk show apical rings and micronemes in (A), respectively. White arrows show central microtubules in (A) and (B).

second dimension at 200 V constant voltage. Second-dimension gels were blotted, and the blotted membranes were immunostained as described above.

Immunoelectron microscopy (*IEM*)

C. parvum sporozoites treated by 0·1% Triton X-100 (Sigma-Aldrich Co.) in RPMI medium 1640 (Invitrogen) in 5–10 min were fixed in 2% PFA in 0·1 M PB at 4 °C for 4–6 days, washed and re-suspended in UPW. Parasites settled on grids were air-dried as described above, stained with anti-α tubulin antibody or normal mouse IgG, the same as IFA. After washing with PBST 3 times, grids were incubated with the secondary antibody, rabbit anti-mouse IgG-conjugated with 5 nm colloidal gold (EY Laboratories Inc.) or goat anti-mouse IgG conjugated with ultra small gold (Electron Microscopy Sciences) for 30 min, and then washed 3 times with PBST and UPW. Silver enhancement was carried out using GoldEnhance™ LM/Blot Formulation (Nanoprobes Inc.) for 1 min according to the manufacturer's protocol. They were washed with UPW, stained by 2% PTA and examined with an electron microscope (H-7500, Hitachi).

RESULTS

Two outer membranes, including the plasma membrane and inner membrane complex, were present throughout the entire region of *C. parvum* sporozoites (Fig. 1A–E). At the apical end of sporozoites, 3 apical rings (Petry and Harris, 1999), an electron-dense collar (Fayer *et al*. 1997), single rhoptry, many micronemes and dense granules were observed (Fig. 1A–D). Furthermore, 2 central microtubules were observed further inside the sporozoites, at approximately 25 nm thickness, and extended from the apical rings of sporozoites (Fig. 1A, F). Between the plasma membrane and inner membrane complex, there were structures previously reported as longitudinal ridges (Uni *et al*. 1987) from the apical region of sporozoites to the posterior at intervals of 30–60 nm, and were approximately 15–20 nm thickness and often observed as spiral around sporozoites in traverse sections (Fig. 1D, E, G, H).

In a preliminary examination of extraction by Triton X-100, only a few sporozoites greatly changed in form were observed, and many oocyst walls with 0·5% concentration of Triton X-100 (data not shown). Under this condition, sporozoites of *C. parvum* were thought to collapse with detergent treatment of Triton X-100; however, the organization of the cytoskeleton was clearly displayed on negatively stained *C. parvum* sporozoites by extraction by 0·1% Triton X-100 in 5 min as a milder condition (Fig. 2A, B). Additionally, without Triton X-100 treatment, no internal organelles of sporozoites were seen because the surface membrane of sporozoites impeded electron microscopic observations (data not shown).

In Fig. 2A, three apical rings and the electron-dense collar below the apical rings were present in the apical region of sporozoites, and micronemes were below the apical region of sporozoites. Furthermore, 2 thick central microtubules were observed inside sporozoites and extended from apical rings to the posterior region (Fig. 2A, B).

We examined the reactivity of anti-α and -β tubulin antibodies with *C. parvum* sporozoites extracted by 0%, 0·1% or 1% Triton X-100 in 10 min. As a result, anti-α and -β tubulin antibodies did not react to any sporozoites treated with 1% Triton X-100 (data not shown). After treatment with 0·1% Triton X-100, anti-α tubulin antibody reacted with the apical tip of sporozoites, and the organelles which extended from the apical to posterior region in sporozoites (Fig. 3A, B). Anti-β

https://doi.org/10.1017/S003118200700385X Published online by Cambridge University Press

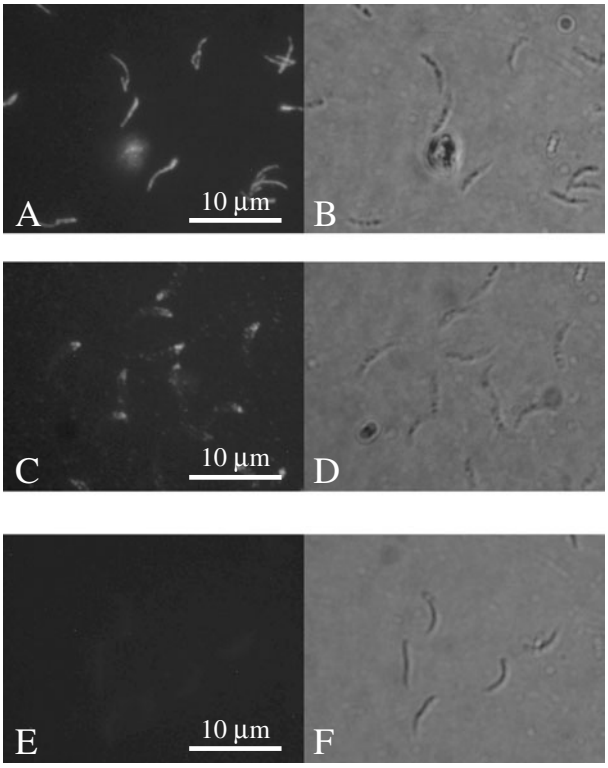

Fig. 3. Immunofluorescence staining of *Cryptosporidium parvum* sporozoites using anti-α tubulin (A and B), anti-β tubulin (C and D) and normal mouse IgG (E and F). Photomicrographs from immunofluorescence microscopy (A, C and E) and bright-field by interference contrast microscopy (B, D and F) are shown.

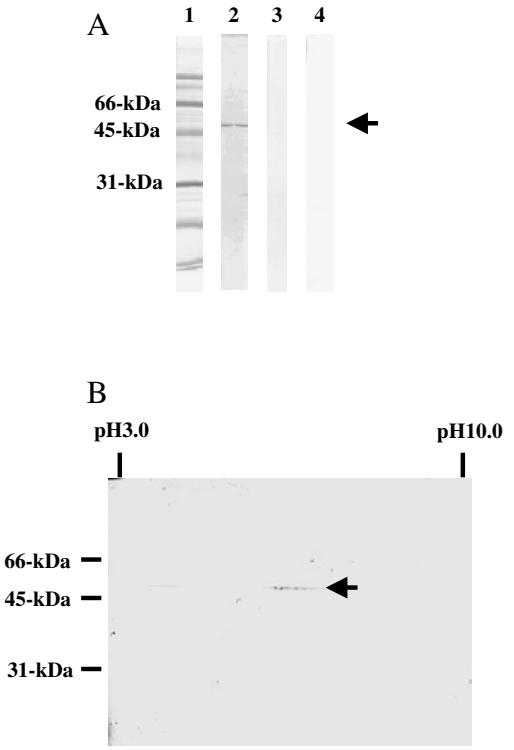

Fig. 4. (A) Western blot analysis probed with the following primary antibodies using 20 μg of *Cryptospoidium parvum* antigens. Lane 2, anti-α tubulin; lane 3, anti-β tubulin; lane 4, normal mouse IgG. Lane 1 shows molecular weight standards. (B) Immunoblot analysis of 20 μg of *C. parvum* antigens with anti-α tubulin antibody by 2-dimensional gel electrophoresis. The left lane shows molecular weight standards. pH values are indicated at the top.

tubulin antibody reacted with only the apical region of sporozoites (Fig. 3C, D) although the reaction of anti-β tubulin antibody was very weak. Normal mouse IgG did not show any reactions with sporozoites (Fig. 3E, F). Without Triton X-100 treatment, there was less reaction of these antibodies with *C. parvum* sporozoites than with 0·1% Triton X-100 (data not shown). When fixed with methanol or acetone, or non-fixed, these reactions were not changed; however, strong non-specific reactions were observed on sporozoites when fixed with 0·05% GA and 2% PFA (data not shown).

Western blotting analysis showed that anti-α tubulin antibody reacted with the 50 kDa *C. parvum* antigens, but anti-β tubulin antibody and normal mouse IgG did not react with any bands (Fig. 4A). Further 2-DE analysis revealed that the α tubulin antigen of *C. parvum* was detected in a pH range of 6 to 7 (6·24) (Fig. 4B).

We tried to stain sporozoites extracted by Triton X-100 using anti-α tubulin antibody in IEM because anti-β tubulin antibody weakly reacted with *C. parvum* zoites in IFA. Consequently, a secondary antibody labelled with 5 nm gold particles failed to penetrate the surface of detergent-extracted sporozoites (data not shown), while ultra-small gold particles were successfully visible on the internal

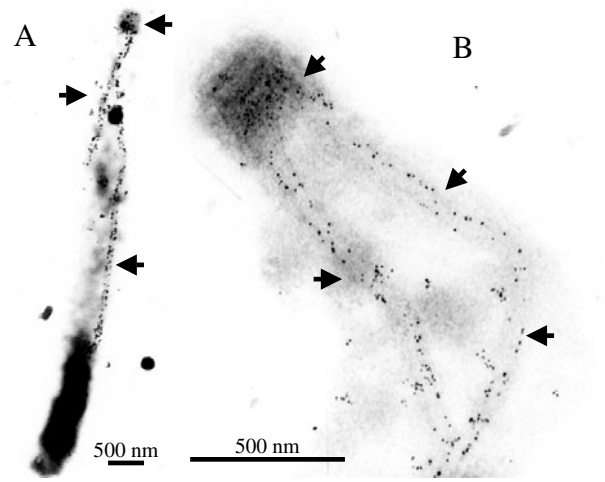

Fig. 5. Immunogold labelling of detergent-treated *Cryptosporidium parvum* sporozoites using anti-α tubulin antibody. Ultra-small gold particles were made visible by silver enhancement. Arrows show structures labelled with gold particles (A and B). (B) Higher magnification of apical region of sporozoites.

organelles after enhancement with silver. The silver-enhanced gold particles were observed on 3 apical rings, the electron-dense collar of the apical region

https://doi.org/10.1017/S003118200700385X Published online by Cambridge University Press

and 2 central microtubules, but not other organelles (Fig. 5A, B), although there were less gold particles on the apical rings and the electron-dense collar than on the 2 central microtubules.

DISCUSSION

To date, there have been many reports about ultrastructural analyses of apicomplexan parasites such as *Plasmodium* spp., *Toxoplasma gondii*, or *Eimeria* spp. (Aikawa, 1971; Dubremetz and Elsner, 1979; Lindsay *et al*. 1991; Tetley *et al*. 1998; Hu *et al*. 2002). Zoites in invasive stages of these parasites have a collection of unique organelles, termed the apical complex, which include rhoptries, micronemes, dense granules, apical or polar rings, conoid and/or subpellicular microtubules; however, as not all apicomplexan zoites possess all these organelles in the apical region, the detailed ultrastructure of zoites of each species is different (Morrissette and Sibley, 2002). For example, conoid was not found in *Plasmodium* spp. and *Theileria* spp., and subpellicular microtubules were not found in *Theileria* spp. (Morrissette and Sibley, 2002). Compared with well-analysed apicomplexan parasites, the ultrastructure of *Cryptosporidium* zoites remains unclear. Thus, the invasive process of *C. parvum*, including the role of the apical complex, is also poorly understood. In the present study, our results showed that *C. parvum* sporozoites possessed secretory organelles, a single rhoptry (2 rhoptries in *Toxoplasma gondii* tachyzoites), multiple micronemes and dense granules around its apical region, and supported the findings reported previously (Tetley *et al*. 1998).

For cytoskeletal organelles of *C. parvum* sporozoites, we could observe 3 apical rings and an electron-dense collar that were present only at the apical end, and 2 central microtubules in the centre of sporozoites but not in other organelles. Therefore, we clarified that it might not possess structures such as subpellicular microtubules surrounding zoites, as in *Toxoplasma gondii*. In addition, many longitudinal ridges were seen in the entire region of *C. parvum* sporozoites between the two outer membranes. These ridges may provide support in the absence of subpellicular microtubules to organize the elongated body shape of sporozoites.

Anti-α and -β tubulin antibodies, which were generated from tubulin origins derived from sea urchin and rat brain, respectively, showed cross-reactivity with *C. parvum* sporozoites in IFA; however, by Western blotting analysis, only anti-α tubulin antibody recognized the approximately 50 kDa antigen of *C. parvum*. Although anti-β tubulin antibody recognized the 55 kDa antigen derived from vertebrates (Gozes and Barnstable, 1982), β tubulin of *C. parvum* might have structurally different carbohydrate modifications on the epitope from those of other origins, while the molecular weight of α tubulin antigen of *C. parvum* coincided with that predicted from the isolated *C. parvum* α tubulin gene (Bonafonte *et al*. 1999) and that of α tubulin from other species (Piperno *et al*. 1987). Furthermore, IEM indicated that cytoskeletal organelles of *C. parvum* sporozoites, including apical rings, the electron-dense collar in the apical region and 2 central microtubules were formed by α tubulin. Our results suggested that α and β tubulins were phenotypically present on *C. parvum* sporozoites, and these cytoskeletons of *C. parvum* sporozoites could possess a conserved function such as motility by polymerization of tubulins, similar to tubulins of other species during the process of host cell invasion.

In conclusion, *C. parvum* sporozoites have a unique apical structure which is different from other apicomplexan parasites. Although the invasion process of *C. parvum* has not been fully elucidated, these characteristics may be related to the extracytoplasmic development of *C. parvum*, which only enter epithelial cells. Although more detailed analysis is needed to clarify these functions during attachment or invasion into host cells, our results are helpful to understand the invasive process of *C. parvum* sporozoites.

This work was partly supported by the Public Trust for Home Economics Research Support Fund (to M.M.).

REFERENCES

Abe, N., Kimata, I. and Iseki, M. (2002). Identification of genotypes of *Cryptosporidium parvum* isolates from a patient and a dog in Japan. *Journal of Veterinary Medical Science* **64**, 165–168.

Abrahamsen, M. S., Templeton, T. J., Enomoto, S., Abrahante, J. E., Zhu, G., Lancto, C. A., Deng, M., Liu, C., Widmer, G., Tzipori, S., Buck, G. A., Xu, P., Bankier, A. T., Dear, P. H., Konfortov, B. A., Spriggs, H. F., Iyer, L., Anantharaman, V., Aravind, L. and Kapur, V. (2004). Complete genome sequence of the apicomplexan, *Cryptosporidium parvum*. *Science* **304**, 441–445.

Aikawa, M. (1971). Parasitological review. *Plasmodium*: the fine structure of malarial parasites. *Experimental Parasitology* **30**, 284–320.

Ashley, E., McGready, R., Proux, S. and Nosten, F. (2006). Malaria. *Travel Medicine and Infectious Disease* **4**, 159–173.

Black, M. W. and Boothroyd, J. C. (2000). Lytic cycle of *Toxoplasma gondii*. *Microbiology Molecular Biology Reviews* **64**, 607–623.

Bonafonte, M. T., Garmon, D. and Mead, J. R. (1999). Characterization of an alpha-tubulin gene of *Cryptosporidium parvum*. *Journal of Eukaryotic Microbiology* **6**, 545–547.

Chen, X. M., Keithly, J. S., Paya, C. V. and LaRusso, N. F. (2002). Cryptosporidiosis. *New England Journal of Medicine* **346**, 1723–1731.

Daugschies, A. and Najdrowski, M. (2005). Eimeriosis in cattle: current understanding. *Journal of Veterinary Medicine and Infectious Diseases and Veterinary Public Health* **52**, 417–427.

Dubremetz, J. F. and Elsner, Y. Y. (1979). Ultrastructural study of schizogony of *Eimeria bovis* in cell cultures. *Journal of Protozoology* **26**, 367–376.

Fayer, R., Speer, C. A. and Dubey, J. P. (1997). General biology of *Cryptosporidium*. In Cryptosporidium *and Cryptosporidiosis* (ed. Fayer, R.), pp. 1–41. CRC Press, Florida, USA.

Gozes, I. and Barnstable, C. J. (1982). Monoclonal antibodies that recognize discrete forms of tubulin. *Proceedings of the National Academy of Sciences, USA* **79**, 2579–2583.

Hanaichi, T., Sato, T., Iwamoto, T., Malavasi-Yamashiro, J., Hoshino, M. and Mizuno, N. (1986). A stable lead by modification of Sato's method. *Journal of Electron Microscopy* **35**, 304–306.

Hu, K., Roos, D. S. and Murray, J. M. (2002). A novel polymer of tubulin forms the conoid of *Toxoplasma gondii*. *Journal of Cell Biology* **156**, 1039–1050.

Laemmli, U. K. (1970). Cleavage of structural proteins during the assembly of the head of bacteriophage T4. *Nature, London* **227**, 680–685.

Lindsay, D. S., Blagburn, B. L. and Toivio-Kinnucan, M. (1991). Ultrastructure of developing *Isospora suis* in cultured cells. *American Journal of Veterinary Research* **52**, 471–473.

Lindsay, D. S., Speer, C. A., Toivio-Kinnucan, M. A., Dubey, J. P. and Blagburn, B. L. (1993). Use of infected cultured cells to compare ultrastructural features of *Neospora caninum* from dogs and *Toxoplasma gondii*. *American Journal of Veterinary Research* **54**, 103–106.

Matsubayashi, M., Kimata, I., Iseki, M., Lillehoj, H. S., Matsuda, H., Nakanishi, T., Tani, H., Sasai, K. and Baba, E. (2005). Cross-reactivities with *Cryptosporidium* spp. by chicken monoclonal antibodies that recognize avian *Eimeria* spp. *Veterinary Parasitology* **128**, 47–57.

Morris, G. M. and Gasser, R. B. (2006). Biotechnological advances in the diagnosis of avian coccidiosis and the analysis of genetic variation in *Eimeria*. *Biotechnology Advances* **24**, 590–603.

Morrissette, N. S. and Sibley, L. D. (2002). Cytoskeleton of apicomplexan parasites. *Microbiology and Molecular Biology Reviews* **66**, 21–38.

Nichols, B. A. and Chiappino, M. L. (1987). Cytoskeleton of *Toxoplasma gondii*. *Journal of Protozoology* **34**, 217–226.

O'Donoghue, P. J. (1995). *Cryptosporidium* and cryptosporidiosis in man and animals. *International Journal for Parasitology* **25**, 139–195.

Perryman, L. E., Kapil, S. J., Jones, M. L. and Hunt, E. L. (1999). Protection of calves against cryptosporidiosis with immune bovine colostrums induced by a *Cryptosporidium parvum* recombinant protein. *Vaccine* **17**, 2142–2149.

Petry, F. and Harris, J. R. (1999). Ultrastructure, fractionation and biochemical analysis of *Cryptosporidium parvum* sporozoites. *International Journal for Parasitology* **29**, 1249–1260.

Piperno, G., LeDizet, M. and Chang, X. J. (1987). Microtubules containing acetylated alpha-tubulin in mammalian cells in culture. *Journal of Cell Biology* **104**, 289–302.

Sagodira, S., Buzoni-Gatel, D., Iochmann, S., Naciri, M. and Bout, D. (1999). Protection of kids against *Cryptosporidium parvum* infection after immunization of dams with CP15-DNA. *Vaccine* **17**, 2346–2355.

Sam-Yellowe, T. Y. (1996). Rhoptry organelles of the Apicomplexa: their role in host cell invasion and intracellular survival. *Parasitology Today* **12**, 308–316.

Tetley, L., Brown, S. M., McDonald, V. and Coombs, G. H. (1998). Ultrastructural analysis of the sporozoite of *Cryptosporidium parvum*. *Microbiology* **144**, 3249–3255.

Uni, S., Iseki, M., Maekawa, T., Moriya, K. and Takada, S. (1987). Ultrastructure of *Cryptosporidium muris* (strain RN 66) parasitizing the murine stomach. *Parasitology Research* **74**, 123–132.

Wiest, P. M., Dong, K. L., Johnson, J. H., Tzipori, S., Boeklheide, K. and Flanigan, T. P. (1994). Effect of colchicine on microtubules in *Cryptosporidium parvum*. *Journal of Eukaryotic Microbiology* **41**, 66.

Xiao, L., Fayer, R., Ryan, U. and Upton, S. J. (2004). *Cryptosporidium* taxonomy: recent advances and implications for public health. *Clinical Microbiology Reviews* **17**, 72–97.